13th International Brick and
Block Masonry Conference
Amsterdam, July 4-7, 2004

EXPERIMENTAL APPROACHES TO THE COMPRESSIVE RESPONSE OF SOLID CLAY BRICK MASONRY

Antonio Brencich[1], Christian Corradi[2], Enrico Sterpi[3]

Abstract

The solid clay brickwork of a 150 years-old bridge is studied through a compressive test on cylinders (ϕ = 150 mm) proposed by UIC (Union Internationale des Chemins de Fer) and flat jacks. FEM analyses, showing the stress distribution inside the specimen, explain the activation, inside the cylinder, of a sand-glass shaped core bearing the applied load, which makes the collapse mechanism of the UIC test partially different from the observed mechanisms for solid clay brickwork. The test results are compared to classical approaches and to other experimental data showing that the proposed test underestimates the compressive strength of masonry. Besides, the evaluation of the elastic average properties is found to be still an open issue.

Key Words

Solid clay brick masonry; Compressive strength; Experimental tests; FEM models.

1 Introduction

The crucial point of constitutive and failure models for masonry is the experimental evaluation of the mechanical parameters. For newly built brickwork the task, at least related to compressive strength, cohesion and friction coefficient, can be dealt with in a relatively simple, but expensive, manner by means of specimens specifically produced for experimental testing. The problem becomes more difficult for existing brickwork, for which only non destructive, or moderately destructive tests can be performed. For these reason, deformation and failure theories are needed. Many approaches have been developed with the aim of defining both theoretical and empirical constitutive models and failure criteria on the bases of the mechanical parameters of masonry constituents, i.e. bricks and mortar (Hilsdorf, 1969, Francis, 1971, Khoo and Hendry, 1973, Atkinson and Noland, 1983, Shrive, 1987, among the others).

The basic assumption of the these approaches considers masonry as an unlimited layered continuum in plane strain conditions; due to the elastic mismatch between single constituents, mortar undergoes a 3D compressive stress state while bricks

[1] DISEG - University of Genoa – Italy – brencich@diseg.unige.it
[2] DISEG - University of Genoa – Italy – corradi@diseg.unige.it
[3] DISEG - University of Genoa – Italy – sterpi@diseg.unige.it

experience a compressive-tensile-tensile 3D state. Collapse is assumed to take place when a limit condition is met in the brick, so that the compressive strength of masonry is the value of the compressive stress leading to that limit state.
The actual distribution of stresses in the brickwork is usually assumed uniform for simplicity, but it is non-uniform due to the local stress concentrations induced by masonry intrinsic inhomogeneity. For these reasons, and since theoretical approaches do not give satisfactory estimations of the experimental data, research on this issue is still needed and the experimental approach remains of fundamental importance.
Moderately destructive tests for existing masonry, allowing direct estimation of some mechanical parameters, mainly consist of flat jack tests and direct compressive testing of drilled cylinders. Due to technical problems, the standard diameter of the cylinders is 80-90 mm, which is too small if compared with the dimensions of the brick and of the mortar joints. In order to overcome some limits of the standard tests on drilled cylinders with small diameter, the UIC (1994) refers to drilled cylinders with a 150 mm nominal diameter, 140-145 mm in fact, which are assumed to represent the actual brickwork.
In this work, experimental compressive tests are carried out on cylinders (ϕ = 150 mm) drilled from the piers of an 150-years old railway bridge. The outcomes, along with the observed collapse mechanisms, are compared to the data from flat jack tests and to FEM analyses. Discussion is carried out on the local concentration of stresses due to the test setup and the non-symmetry of the cylinder, and on the collapse mechanism reproduced by the UIC test. The experimental results and the UIC approach are compared to classical approaches and to other experimental data giving an estimate of the reliability of the proposed UIC test.

2 UIC compressive test and experimental setup

The UIC proposal asks the cylinder (150 mm in diameter) to present a vertical joint and two horizontal joints in the centre of the section, figure 1. The specimen is loaded on the longitudinal direction, and both the vertical and horizontal displacement are recorded. The compressive strength of brickwork is simply assumed as the ratio between the collapse load and the horizontal cross section, figure 2:

$$f_c = \frac{F_{coll}}{\phi \, l} \tag{1}$$

f_c is the compressive strength;
F_{coll} is the load at collapse;
ϕ and l are the cylinder diameter and length.

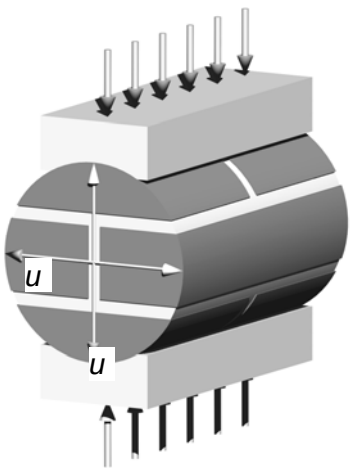

Figure 1 Test arrangement

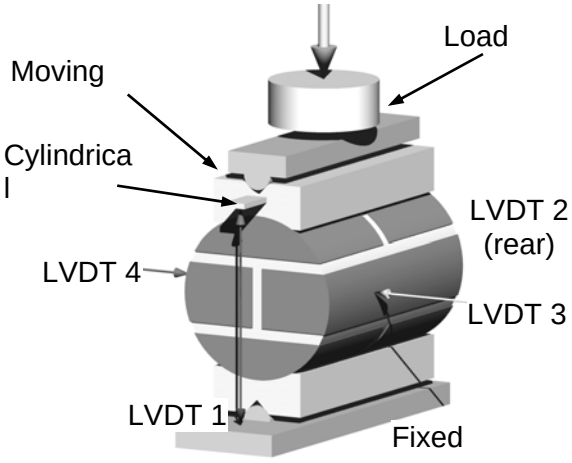

Figure 2 Detail of test arrangement

For the evaluation of the secant elastic modulus and of the strains in the loading direction and in the transversal one, the reference section is assumed as $0.75\phi l$ and the reference loads are at 1/10th ($F^{0.1}$) and 1/2 ($F^{0.5}$) of the limit load. The elastic modulus and the Poisson coefficient are, therefore, obtained by means of simple relations referred to the range [$F^{0.1}$, $F^{0.5}$]:

$$\varepsilon_h = \frac{u_h}{\phi}, \qquad \varepsilon_v = \frac{u_v}{\phi} \tag{2.a,b}$$

$$\Delta\varepsilon_h^{0.1-0.5} = \frac{u_h^{0.5} - u_h^{0.1}}{\phi}, \qquad \Delta\varepsilon_v^{0.1-0.5} = \frac{u_v^{0.5} - u_v^{0.1}}{\phi} \tag{3.a,b}$$

$$E = \frac{4}{3}\frac{F^{0.5} - F^{0.1}}{\left(u_v^{0.5} - u_v^{0.1}\right) l}, \qquad \nu = \frac{u_h^{0.5} - u_h^{0.1}}{u_v^{0.5} - u_v^{0.1}} \tag{4.a,b}$$

ε_v and ε_h are the vertical and horizontal strains respectively;
u_v and u_h are the vertical and horizontal displacements;
F is the recorded loading force;
the apex 0.1 and 0.5 refer to the quantities recorded at $F^{0.1}$ and $F^{0.5}$.

The testing setup is presented in Figure 2; minor details are omitted for simplicity. The load measuring device is a C5 class *HBM-RTN* load cell with a 0.01% precision and is located in-between the upper plate and the testing machine. The upper and lower plates are connected to the testing frame through cylindrical hinges that allow the load line to be precisely identified. The relative displacements are measured by means of HBM LVDTs with a 0.001mm precision. The displacement of the upper plate is measured at the two ends of the specimen (LVDTs n. 1 and 2), while the lateral ones are recorded at the centre of the cylinder (LVDTs n. 3 and 4), so that u_v, eq. (2) and (3), is directly the sum of devices 3 and 4.

The moving end of the machine is displacement controlled, the load being measured by the load cell. In this way, the load process is substantially a displacement-controlled procedure. The load cell can be considered as a spring with high stiffness; up to the limit load this does not affect the results at all; it significantly alters the measurements only far after the material collapse, at a point when the softening curve has already lost any mechanical meaning. A 2 mm thick lead sheet between the specimen and the loading plates was used to regularise the lateral surface of the cylinder.

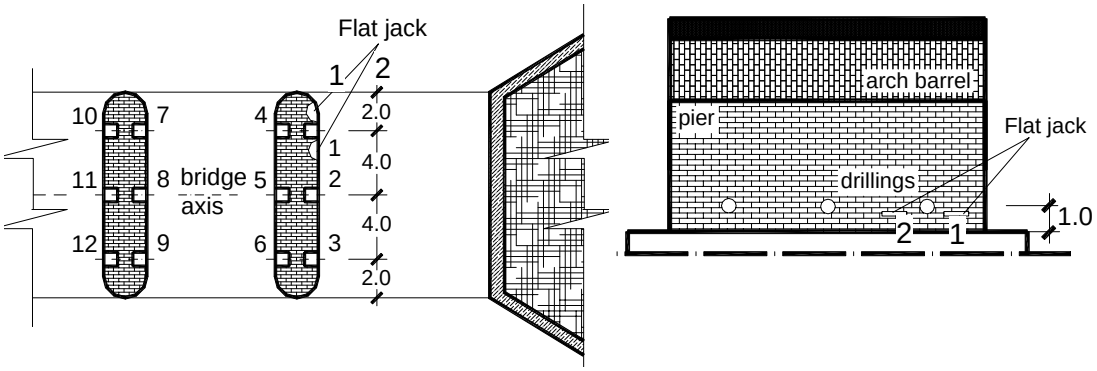

Figure 3 Position of drillings and flat jack: a) horizontal and b) vertical position

3 Test results

The cylindrical specimens have been drilled from two piers of a 150 years old railway bridge in Alessandria, Italy. Figure 3 shows the position of the drillings which can be partially recognized in figure 4 at approx. 1m from the average water level. The studied masonry is typical of the bridges built in the second half of the 19th century, both for the

materials, solid clay bricks and lime mortar, table 1, and for the brickwork bond. Since the mortar could not be tested in standard TPB and direct compression tests, literature data are assumed for the calculations discussed later on.
The cylinders nominal diameter was 150 mm but the external actual diameter was approximately 145 mm, the length being 240 mm. Due to practical problems, not all the specimen were drilled so as to present the mortar joints in the centre of the cross section, as in figure 1; in fact, some of them presented vertical and/or horizontal eccentricity (≈10mm) of the mortar joints, as summarized in table 2.

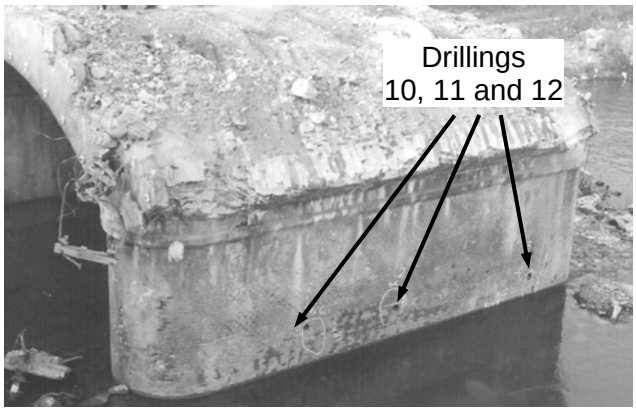

Figure 4 Position of the drillings 10, 11 and 12 in the second pier

Table 1 Material strength and elastic properties

Notes	Value		Property		Value	Notes
Direct compr. on 4 specimen	1500±170	*BRICK*	E [MPa]	*MORTAR*	335	Brencich et al. (2002)
Brencich et al. (2002)	0.05±0.007		ν		0.2	Rots (1991)
Direct compr. on 4 specimen	19.3±2.7		f_c [MPa]		14.7±0.6	Brencich et al. (2002)
TPB – av. 3 specimens	3.9±0.3		f_t [MPa]		1.4	Brencich et al. (2002)

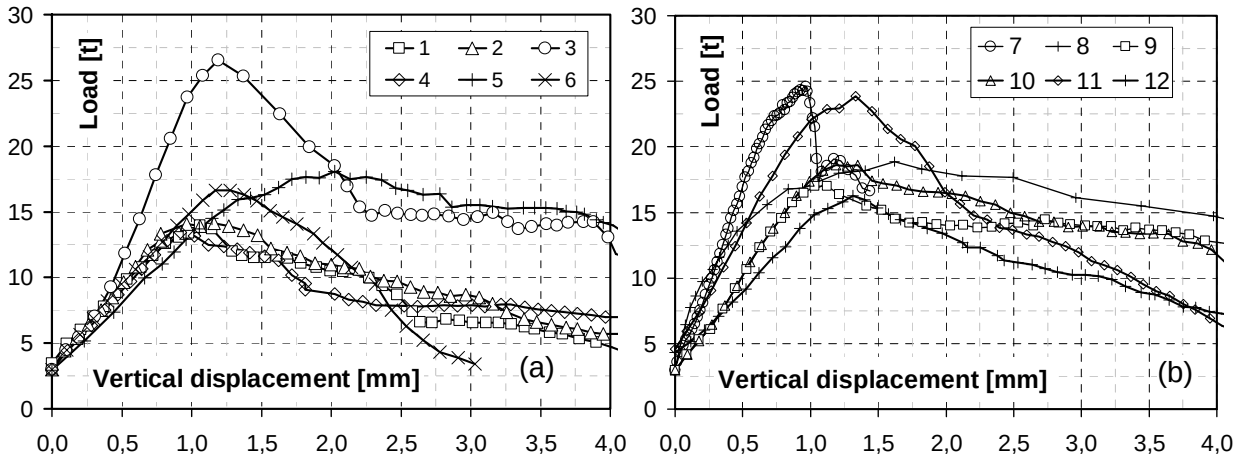

Figure 5 Load-Displacement (vertical) response of specimens a) 1-6, b) 7-12

Figure 5 represents the load-vertical displacement response of the specimens; along with the data of table 2, it can be observed that the results are rather dispersed due to brickwork inhomogeneity. Figures 6 and 7 show the crack pattern during and at the end of the tests; according to the crack pattern, the load seems to be transferred by the central, sand-glass shaped, part of the specimen only, figure 7, and not by the entire section as it is suggested by eq. (1). In fact, at approximately 80% of the maximum

load, cracks appear at the two ends showing both the activation of the sand-glass shaped core and the detachment of the lateral leaves. Besides, in figure 7.b the opening of the central joint can be clearly recognized.

Table 2 Main results of the tests

n.	Notes	F_{coll} [t]	E [MPa] eq. (4.a)	ν eq. (4.b)	f_c [MPa] eq. (1)	ε_{coll} $*10^{-3}$ eq. (2.b)
1	hor. ecc.	13.96	482.5	1.20	3.88	7.4
2	no ecc.	14.09	531.5	0.75	3.91	6.7
3	hor. ecc.	26.52	761.0	0.82	7.37	8.1
4	hor. ecc.	13.41	504.0	0.21	3.72	6.4
5*	vert. and hor. ecc.	18.08	441.0	0.48	5.02	13.8
6	vert. ecc.	16.61	547.5	0.59	4.61	8.1
7	vert. ecc.	24.57	1130.0	0.64	6.82	6.5
8	no ecc.	18.87	510.0	0.44	5.24	11.6
9	hor. ecc.	17.00	585.0	0.59	4.72	7.7
10	vert. ecc.	18.60	584.0	0.60	5.17	8.1
11	vert. ecc.	23.85	742.5	0.59	6.62	9.2
12	no ecc.	16.25	385.0	1.07	4.51	9.2

*: specimen n. 5 showed completely different bricks (lighter red) than the others

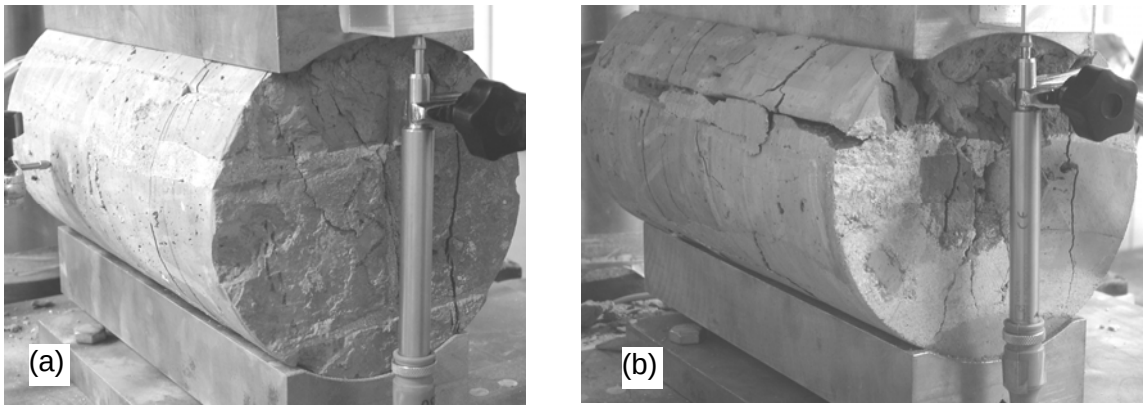

Figure 6 Specimen 7: crack pattern at a) 80% of the maximum load; b) the end of the test

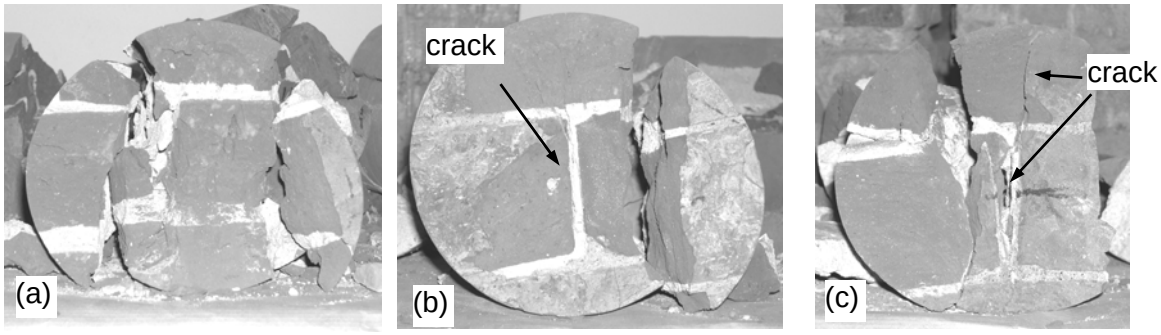

Figure 7 Specimens 9, 10 and 12 at the end of the test

Table 2 shows the experimental data from which we can observe that: a) the compressive strength appears to be rather low; b) the calculated values for the Poisson ratio are unacceptable. All these circumstances will be discussed in the concluding section on the bases of the FEM models presented in the next paragraph.
Figure 8 presents the results of the flat jack tests; the diagrams refer to the upper values of the cyclic loading only; in both the cases the compressive strength appears to

be around 7.4 MPa, even though the stress-strain curves seem to indicate a somewhat higher strength.

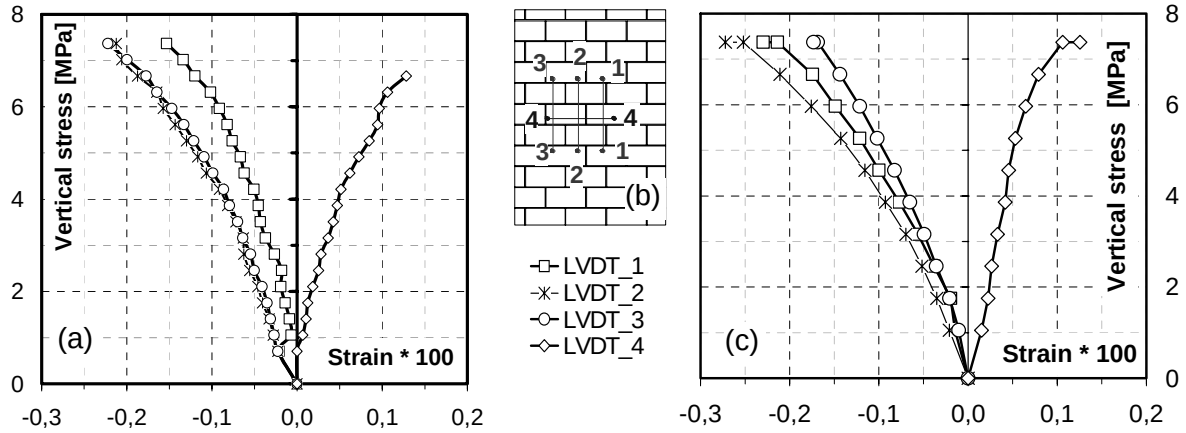

Figure 8 Stress-Strain curves (maximum only) for the two flat-jack tests: a) flat jack 1; b) distribution of the LVDTs; c) flat jack 2

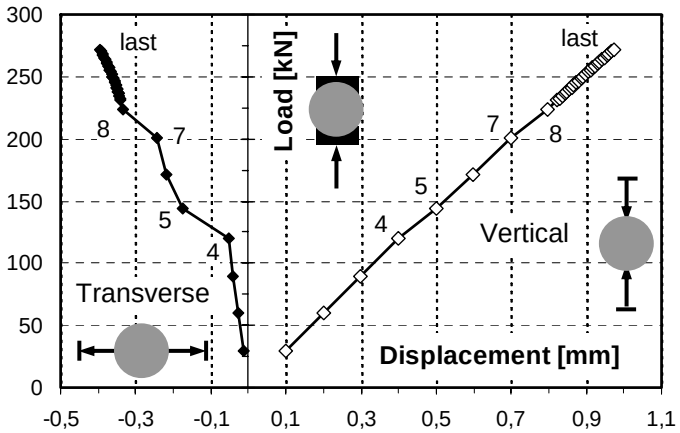

Figure 9 Load-Displacement response of the numerical model. Right: vertical displacement – Left: transverse displacement

4 FEM models

FEM models are able of enlightening some aspects of the mechanical response of masonry-like structures only in the first stage of the loading process. Since masonry undergoes large cracking far before the collapse load is reached, these models fail in predicting the ultimate load. Nevertheless, they can be used to understand the activation of cracking and the first steps of its evolution. For these reasons, a FEM model was formulated assuming the mechanical parameters of Table 1. Since no direct testing was possible on mortar, some data are assumed from related literature.

The 3D FEM model represented the whole of the specimen, the lead leaves used to distribute the load on the lateral surface and the loading plates, and consists of 6080 solid elements with second order shape functions, 7337 nodes accounting for 22011 d.o.f. The constitutive model for masonry is that of a brittle isotropic material with a tensile strength of 3.9 MPa; the compressive strength of 19 MPa was, in fact, never reached since the crack propagation made the numerical procedure to stop before the maximum compressive stresses was attained. The FEM model can be deduced from the following figures, all representing the central cross section of the specimen.

Figure 9 shows the load-displacement curve of the FEM model; on the right-hand side

the load-vertical displacement curve shows that the activated cracking is not enough to make the specimen exhibit a macroscopic non linear behaviour, whilst the lateral displacement, left-hand side of figure 9, shows a curve with two distinct parts: at step 4 the stiffness suddenly decreases as cracking is activated; than the stiffness remains approximately constant at the reduced value while cracks propagate. Figure 10 shows the evolution of cracking inside the cylinder as the load increases. It can be clearly recognized the gradual activation of the central sand-glass shaped core of brickwork that had been already detected during the tests; the sudden increase of the lateral displacement seems to be due to the opening of the central joint, figure 7.b,

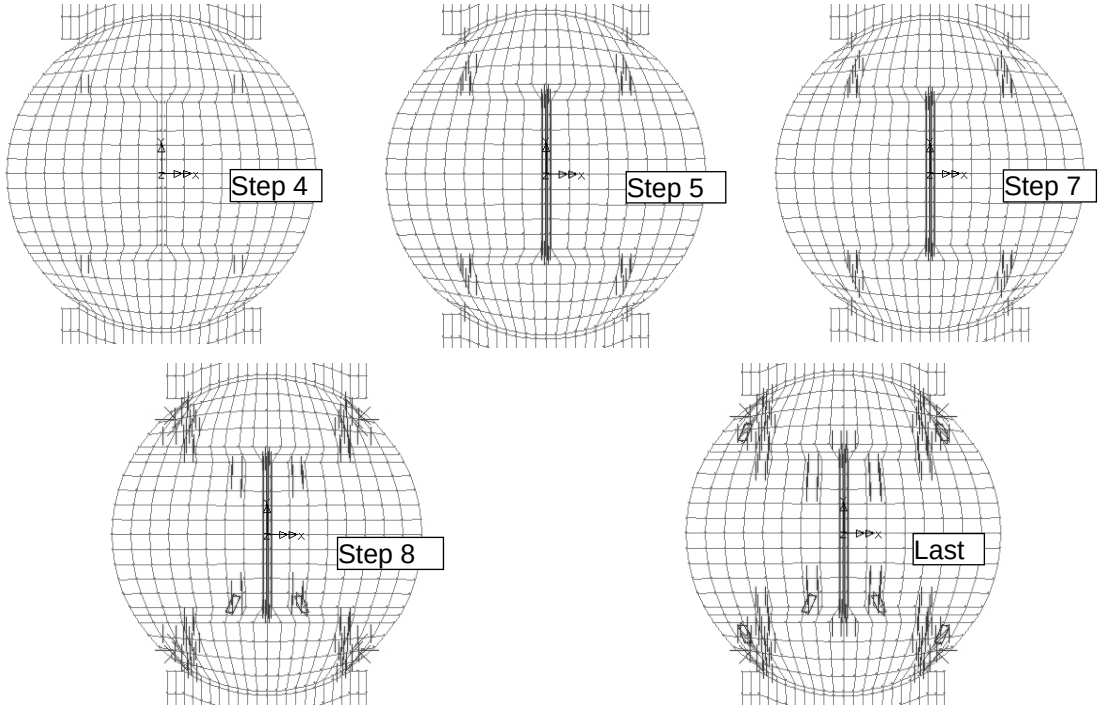

Figure 10 Crack pattern evolution during the load process (see fig. 9)

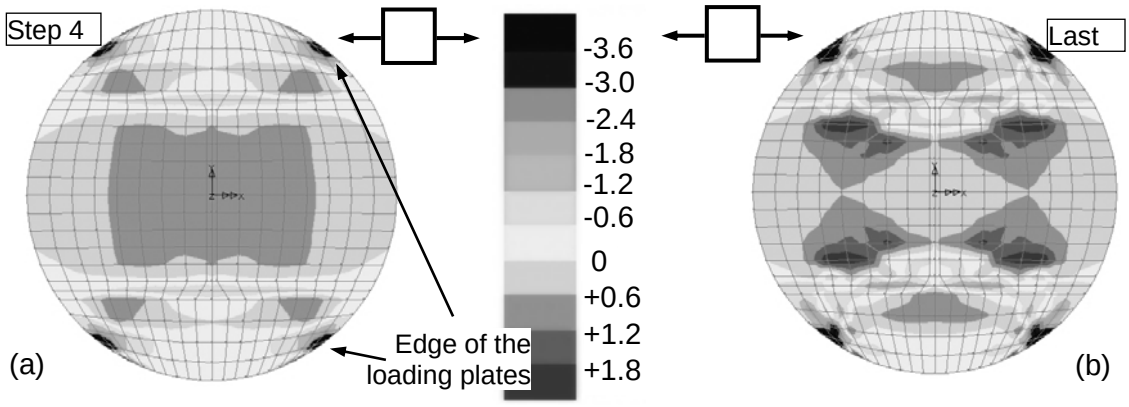

Figure 11 Transverse stresses [MPa] at: a) step 4; b) last step

Figure 11 shows the transverse stresses at step 4 and at the last step. The distribution of tensile stresses is in agreement with the observed crack pattern, showing also a strong local effect, stress concentration, at the edges of the loading plates which is responsible for the detachment of the lateral parts of the cylinders (figures 6.b and 7).
Figure 12 displays the distribution of the vertical stresses at the same two steps: while at the beginning of the load history, figure 12.a, the central sand-glass shaped core is rather wide, at the final step its load-bearing part, the inner one, is reduced to

approximately 1/3rd of the whole cross section.

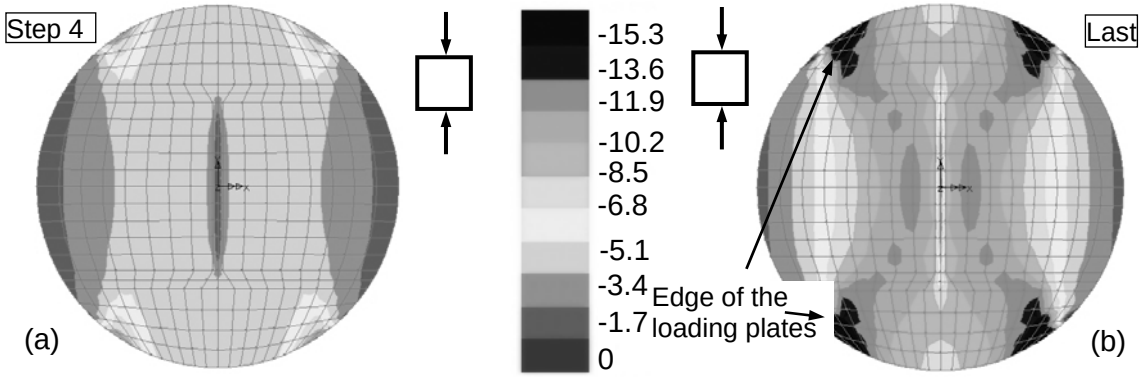

Figure 12 Vertical stresses [MPa] at: a) step 4; b) last step

5 Comparisons and discussion

Since the studied brickwork had been taken from the piers of an existing bridge, no data are available on mortar; according to literature data on historical lime mortars, we can assume its compressive strength to be inside the range 8-12 MPa. Besides, the experimental outcomes cannot be compared to the compressive strength measured on prismatic specimens because only cylinders had been taken from the bridge. For this reason, we will refer to the compressive strength of the tested brickwork estimated on the bases of well known theories and on code-type approaches. In the latter case, it has to be noted that codes usually give characteristic values of the strength, while the comparison with experimental data should be carried out on the average values. For this reason, we assume that the average values for compressive strength can be derived multiplying the code-type estimates by a factor 1.2 (EN1052-1, 1998). Table 3 shows the estimated values for the compressive strength for the cases of mortar exhibiting a compressive strength of both 8 and 12 MPa, the latter values being in parenthesis.

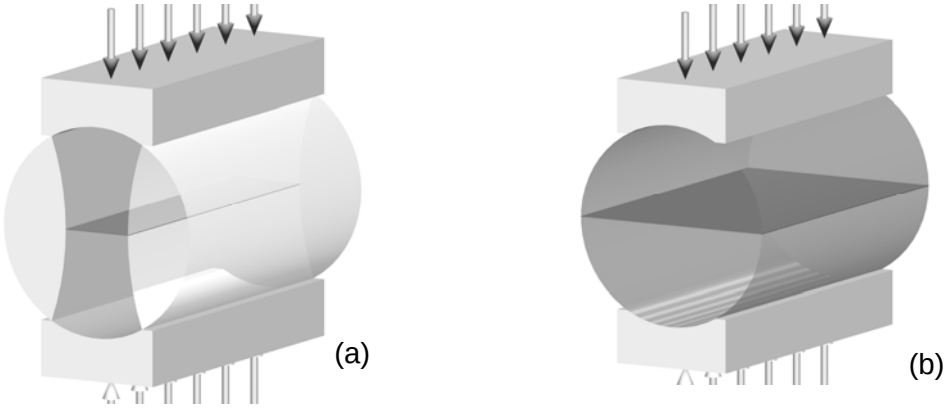

Figure 13 Actual load bearing section: a) experimental evidence; b) according to eq. (1)

The experimental data account for an average compressive strength of 4.5 MPa (not considering the extreme values). Figure 12.b shows that the actual load-bearing central core, according to the experimental evidences of figure 7, is approximately half of the nominal cross section, figure 13.a. Taking into account the distribution of the compressive stresses in this inner part of the specimen, we can say that formula (1), referring to the section of figure 13.b, underestimates the actual compressive strength by a factor of approximately 1.7; introducing this correcting factor the experimental

value of the compressive strength would be 7.6 MPa, so that good agreement is found with the estimated values given by experimental approaches and code-type provisions.
The elastic approach by Francis et al. (1971) and the simplified formulas by Fiche-UIC (1994) and by Euro Code 6 (1998, 2002) allow an estimation of the elastic modulus; table 4 compares the estimates with the average experimental value. It can be seen that the data are quite disperse, showing that a reliable estimate of the elastic modulus is not easy to be defined for masonry.

Table 3 Compressive strength of brickwork

	Reference	Notes	Compressive strength [MPa]	
Analytical + Experimental	Francis et al. (1971)	elastic theory	13.9 (13.9)	
	Hilsdorf (1969)	limit analysis	12.2 (12.4)	
	Khoo & Hendry (1973)	limit analysis + experimental	8.4(12.3)	
	Tassios (1987)	Experimental	8.2 (8.7)	
	Tassios (1987)	Simplified experimental	6.2 (7.1)	
			Char. value	Av. value
Design codes	Euro Code 6 (1998)	-	5.8 (6.4)	6.9 (7.7)
	Euro Code 6 (2002)	-	6.5 (7.3)	7.8 (8.7)
	Fiche-UIC (1994)	-	5.7(5.8)	6.8(6.9)
	Italian Code (1987)	-	7.0 (8.0)	8.4(9.6)
	BS 5628 (1992)	-	5.0 (7.0)	6.0(8.4)
	Present work experimental	UIC test – eq. (1)	<4.5>	
		UIC test – corrected	7.6	
		flat jack – 2 tests – average	<7.4>	
Compressive strength of the mortar: 8 MPa (In parenthesis the value for a mortar with a 12 MPa compressive strength)				

Table 4 Elastic modulus of brickwork

	Francis et al.(1971)	Fiche-UIC (1994)	EuroCode 6 (2002)	Present work – experimental		
				UIC test	Flat Jack	
E [MPa]	1195	1195	4560	<550>	4350	3460

6 Conclusions

An extensive experimental program on solid clay brick masonry from an existing bridge, on the bases of both the UIC compressive and flat jack test, has been presented; FEM analyses have been used to explain the observed collapse mechanism. The comparisons with the estimates given by theoretical and code-type approaches showed that the UIC test underestimates the compressive strength, approximately 40%, probably because the actual collapse mechanism is affected by local phenomena (sand-glass shaped core of masonry). The correction of the provided formula could give, at least in the studied case, a better estimate of the compressive strength of masonry.
The formulas suggested for the evaluation of the elastic properties, elastic modulus and Poisson ratio, appear to be only a first contribution to the problem of measuring the elastic properties of masonry rather than reliable formulas for professional engineers.

7 Acknowledgements

The authors gratefully acknowledge the contribution of Dott. Ing. Ugo De Francesco and Dott. Ing. Andrea Sereno to the experimental tests.

This research was carried out with the financial support of the (MURST) Department for University and Scientific and Technological Research in the frame of the PRIN 2003/ 2004 Project "*Safety, Conservation and Management of Masonry Bridges*".

References

Atkinson R.H., Noland J.L., 1983, A proposed failure theory for brick masonry in compression, Proc. of the 3rd Can. Mas. Symp., Edmonton.

Brencich A., Corradi C., Gambarotta L., Mantegazza G., Sterpi E., 2002, Compressive strength of solid clay brick masonry under eccentric loading, Proc. Brit. Mas. Soc., **9**, november 2002, 37-46.

BS 5628, Part 1, 1992, Code of practice for use of masonry. Structural use of unreinforced masonry. Part 3, 2001, Code of practice for use of masonry. Materials and components, design and workmanship.

Dept. Publ. Works, 1987, Technical code for design, building and assessment of masonry buildings and their strengthening, (only in Italian).

EN 1052-1, 1998, Methods of test for masonry – Part 1: Determination of compressive strength

ENV 1996-1-1 march 1998 and December 2002 – EURO CODE 6. Design of masonry structures, Part 1-1: General rules for buildings – Rules for reinforced and un-reinforced masonry.

FICHE-UIC 778-3E, 1994, Recommandations pour l'evaluation de la capacite portante des ponts-voutes existants en maçonnerie et beton.

Francis A.J., Horman C.B., Jerrems L.E., 1971, The effect of joint thickness and other factors on the compressive strength of brickwork, Proc. 2nd I. B. MA. C., Stoke on Kent.

Hilsdorf H.K., 1969, Investigation into the failure mechanism of brick masonry under axial compression, in Designing, Eng.ng & Construction with Masonry Products, F.B. Johnson ed., Gulf Publishing, Houston, Texas.

Khoo C.L., Hendry A.W., 1973, A failure criteria for brickwork in axial compression, Proc. 3rd I.B.Ma.C., Essen, 141-145

Rots J.G., 1991, Numerical simulation of cracking in structural masonry, *Heron*, **36**.

Shrive N.G., 1983, 'A fundamental approach to the fracture of masonry', Proc. 3rd Can. Mas. Symp., Edmonton, 4/1-4/16.

Tassios, T.P., 1987, The Mechanics of Masonry, Symmetria Publishing, Athens.

Union Internationale des Chemins de Fer. Fiche UIC_778-3E, 1994, Recommandations pour l'evaluation de la capacite portante des ponts-voutes existants en maçonnerie et beton.